JOURNAL OF APPLIED ELECTROCHEMISTRY 18 (1988) 608–613

Response rate techniques for zirconia-based Nernstian oxygen sensors

S. P. S. BADWAL, M. J. BANNISTER, F. T. CIACCHI

CSIRO, Division of Materials Science and Technology, Normanby Road, Clayton, Victoria, Australia 3168

G. A. HOOSHMAND

Communications Airway Systems Branch, Department of Aviation, PO Box 367, Canberra, ACT, Australia 2601

Received 25 October 1987; accepted 17 February 1988

Several techniques are described to determine the rate of response of electrodes used in Nernstian sensors to oxygen concentration changes in various environments. These techniques are related to combustion control and automotive applications as well as laboratory testing of electrodes. The response behaviour of the electrodes used in the $SIRO_2$ low temperature sensor has been characterized and comparison made with several other electrodes used conventionally in oxygen sensors.

1. Introduction

Oxygen sensors are commonly used for (i) process control in chemical and metallurgical industries and (ii) better fuel efficiency and reduced emission levels in automobiles and industrial boilers. In these applications the sensor is used in a controlled loop feedback system. The sensor is placed either downstream or in the process environments to monitor the oxygen activity. The EMF signal generated by the sensor is fed back to the controller for optimization of the process or combustion conditions. For the controlled loop feedback system to work efficiently, the inherent speed of response of the sensor to fluctuations in the oxygen concentration plays an important role. Several techniques have been under investigation in this laboratory to monitor the rate of response of Nernstian sensors to changes in oxygen concentration in various environments.

This paper discusses the merits and limitations of the techniques, and describes results obtained for the low temperature response of electrodes used in Nernstian sensors.

2. Response rate techniques

2.1. *Differential response technique*

This method involves simultaneously exposing both electrodes of a solid electrolyte cell based on stabilized zirconia to a sudden change in the oxygen concentration. If the two electrodes respond at different rates, an EMF is developed. The sign and shape of the EMF–time curve provides useful information on the relative speed of both electrodes. The technique is semi-quantitative and most suitable for comparing the response of one electrode against another [1].

2.2. *Nernstian response technique*

The technique involves exposing one electrode of a zirconia-based Nernstian oxygen sensor to a reference gas and changing the atmosphere at the other electrode between two gases having different oxygen partial pressure. The method is useful for determining the intrinsic response of a single electrode at a time. Only a few authors have reported response rate data using this technique [2–5].

2.3. *Two-burner response technique*

The response rate techniques described above involve the use of well-characterized gases such as air and oxygen/nitrogen mixtures. While these techniques are useful for comparing and measuring the response behaviour of various electrodes, they do not simulate the complex environments usually experienced by the sensor electrodes. Sensors commonly encounter combustion product mixtures from boiler flues and car exhausts which contain nitrogen, oxides of nitrogen, water vapour and carbon dioxide plus, in many cases, traces of combustibles such as carbon monoxide and unburnt hydrocarbons. A burner technique is more appropriate for such applications.

In the literature most of the response rate data for combustion product mixtures has been reported for a single burner system [6–8]. With this type of response rate rig uncertainties are introduced because of the time lag between the burner and the sensor location, and because of the new gas front mixing with the previous gas composition delivered by the burner. These uncertainties are considerably reduced in the two-burner arrangement used in this laboratory [9]. The method involves exposing one side of the zirconia Nernstian oxygen sensor to a reference gas and rapidly

0021-891X/88 $03.00 + .12

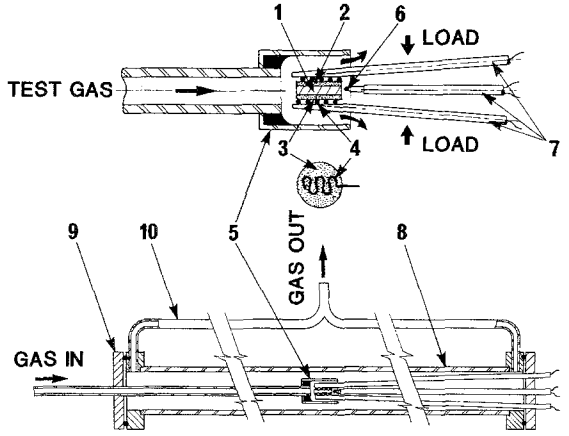

Fig. 1. Differential response rate assembly. (1) Electrolyte, (2) reference electrode, (3) test electrode, (4) serpentine Pt connection, (5) gas shroud, (6) thermocouple, (7) twin bore alumina tube, (8) alumina work tube, (9) brass ends, (10) exhaust gas manifold.

changing the atmosphere at the test electrode between the combustion product mixtures from two propane/air burners set to different air/fuel ratios.

3. Experimental details

For the differential response rate technique the test electrode was applied on one flat face of an yttria (7 or 10 mol %)-stabilized zirconia disc (diameter 9–10 mm, thickness 2–3 mm) and given an appropriate heat treatment (see below). The common reference electrode against which all other electrodes were compared was then painted on the other flat face of the electrolyte disc. The reference electrode (PtU2B) was a mixture of platinum and a urania–scandia fluorite-type solid solution (75 wt % $(U_{0.38}Sc_{0.62})O_{2\pm x}$ + 25 wt % PtO_2) developed for low temperature operation of the $SIRO_2$ sensor [10, 11]. The test electrodes included: PtU2B; platinum pastes 8907 and 6082 (from Engelhard Industries); sputtered Pt (0.4 μm thick) heat treated at 600° C (100 h), 750° C (75 h), 900° C (2 h) or 900° C (50 h); PtX1 (75 wt % $(U_{0.4}Pr_{0.6})O_{2\pm x}$ + 25 wt % PtO_2) and a co-sintered urania–scandia electrode described previously [12, 13] and almost blocking to the oxygen transfer reaction. The latter electrode was prepared by co-sintering a thin layer of $(U_{0.38}Sc_{0.62})O_{2\pm x}$ electrode on 10 mol % Y_2O_3–ZrO_2 electrolyte at 1400° C. Because of the formation of a dense intermediate layer, as a result of reaction between yttria–zirconia and a volatile uranium-containing species produced by decomposition of the urania–scandia electrode, the rate of the oxygen exchange reaction at the interface is extremely slow. The differential response rate cell assembly is schematically shown in Fig. 1.

For the Nernstian response technique the sensor bodies were prepared by forming a ceramic weld at high temperatures between an alumina tube and a solid electrolyte disc or pellet consisting of 50 wt % (yttria–zirconia or scandia–zirconia) + 50 wt % alumina [11]. In the high temperature sensor a pellet of yttria–zirconia and in the low temperature sensor assembly a scandia–zirconia disc was used as the solid electrolyte. Complete sensors were made by painting both sides of the electrolyte disc or pellet with the PtU2B electrode and assembling the various sensor components as shown in Fig. 2a. The sensor assembly was placed inside a controlled atmosphere housing (Fig. 2b). The step change in the oxygen partial pressure was confined to the inner electrode of the sensor while the oxygen concentration at the outer electrode was maintained at a constant level by reference air.

In this technique and the previous differential method the gas displacement volume in the cell chamber was less than 3 cm^3 and the gas flow rate $\sim$140 $cm^3\,min^{-1}$. For both techniques the changes in test atmosphere were made using fast-acting solenoid valves and the data were collected with a computer controlled data logger over the temperature range 350–600° C.

For the two-burner response method the air/fuel ratio was set separately for each burner with the help of oxygen sensors placed in the exhaust stream as shown in Fig. 3. The combustion product mixture from each burner was fed through separate ducting to the outer electrode of the test sensor, where a fast-acting ($\sim$10 ms) electropneumatic valve deflected one or other exhaust stream over the test sensor. The valve operation as well as data acquisition (at rates up to 40 kHz) were controlled by a computer. The equipment

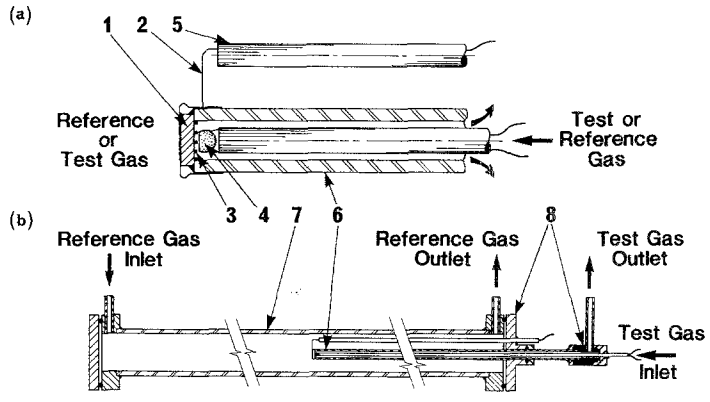

Fig. 2. (a) A schematic diagram of the Nernstian oxygen sensor. (1) Electrolyte, (2) external connection, (3) Pt spiral, (4) thermocouple and internal connection, (5) twin bore alumina tube, (6) alumina tube. (b) Nernstian response rate assembly. (7) Alumina work tube, (8) brass ends.

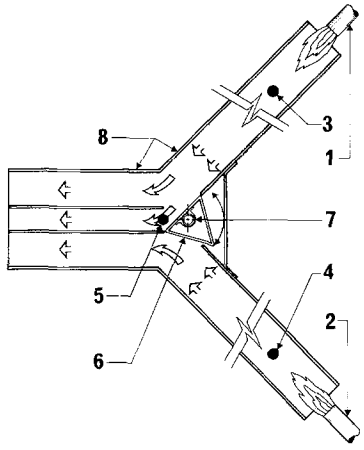

Fig. 3. Two-burner response assembly. (1) Burner No. 1, (2) burner No. 2, (3) monitoring sensor for burner 1, (4) monitoring sensor for burner 2, (5) test sensor, (6) electropneumatically driven deflector, (7) pivot point, (8) stainless steel ducting.

is capable of making measurements either for single step changes in air/fuel ratio or during cycling (at a variable frequency) between the two burners. The inner electrode of the sensor was always exposed to air. The sensors themselves were made as described above, and had electrodes of PtU2B (low temperature sensor) or platinum paste 6082 (high temperature sensor).

4. Results and discussion

4.1. *Differential response rate technique*

Typical experimental EMF–time curves for step changes in oxygen concentration from 1 to 21% and 21 to 1% are shown in Fig. 4 for two cells. The sign of the observed EMF signal determines which of the two electrodes is responding faster. The magnitude of the peak height increases with increase in the difference in the response times of both electrodes. For two identical electrodes on the same disc the magnitude of the differential EMF signal was less than 1 mV. In the case of a blocking electrode/yttria–zirconia/PtU2B cell, the observed EMF signal was close to the value expected when only one electrode of the Nernstian

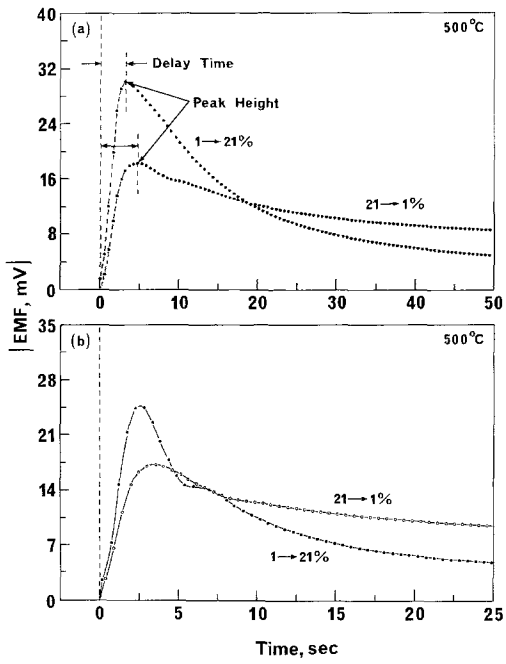

Fig. 4. Differential response curves at 500° C for: (a) PtU2B/yttria–zirconia/sputtered Pt (0.4 μm), 900° C (50 h) cell; (b) PtU2B/yttria–zirconia/sputtered Pt (0.4 μm), 750° C (75 h) cell, subjected to oxygen concentration changes from 21 to 1% and 1 to 21%.

sensor assembly responds to oxygen concentration changes (Fig. 5). For all other test electrodes intermediate values were observed. For sputtered Pt electrodes given different heat treatment, the magnitude of the peak height increased as the microstructure of Pt became coarser (Fig. 6) and the number of active sites for the oxygen transfer reaction decreased (Table 1), thus indicating an increase in the response time of Pt electrodes with high temperature treatment.

The time between the initial change in the cell EMF and the occurrence of the peak maximum (delay time) was influenced by the actual value of the response time of each electrode. Since with decrease in the temperature the response times increase, the delay time for all the cells studied normally increased with decrease in the temperature. The PtU2B electrodes developed for the $SIRO_2$ low temperature sensor responded faster than most of the test electrodes.

Because of the overlap in the responses of the two

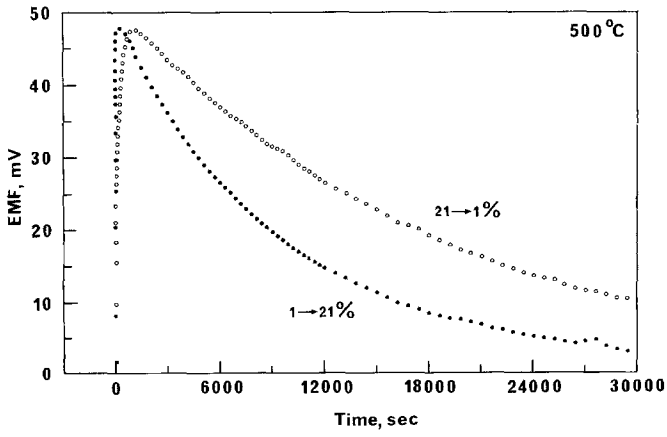

Fig. 5. Differential response curves at 500° C for a PtU2B/yttria–zirconia/cosintered-electrode cell subjected to oxygen concentration changes from 21 to 1% and 1 to 21%.

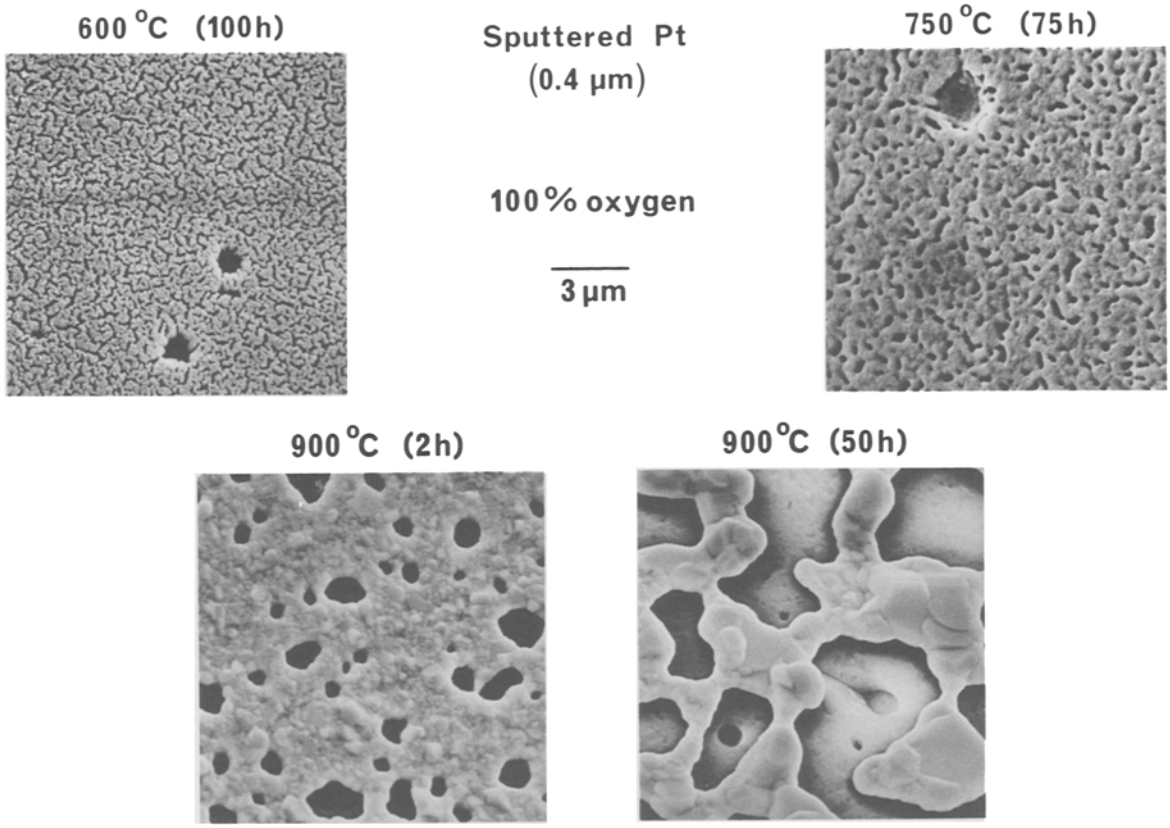

Fig. 6. Scanning electron micrographs of sputtered Pt (0.4 μm thick) on fully stabilized yttria–zirconia substrate given different heat treatments in 100% oxygen.

electrodes and especially when they have complex mathematical relationships between EMF and time, it is difficult to obtain absolute response times for each electrode. The method thus provides only semi-quantitative information. Despite these limitations the differential response rate technique is simple and extremely useful for comparing the response of different electrode materials without the necessity of preparing duplicate Nernstian oxygen sensors with their own separate test and reference gas supplies.

4.2. *Nernstian response technique*

At temperatures above 450° C the intrinsic response of the PtU2B electrode was much faster than the response rate of the Nernstian response rate rig. The data therefore were collected only between 350 and 450° C. Figure 7 shows representative response curves for step changes in the oxygen concentration from 1 to 21% and vice versa. On changing the oxygen concentration from 1 to 21%, the sensor electrode responded faster than when the oxygen concentration was changed from 21 to 1%. The initial rise times for the differential response curves on PtU2B/yttria–zirconia/test electrode cells were similar to those obtained for the PtU2B electrode with the Nernstian response assembly indicating consistency between the two techniques.

Nernstian response data for the PtU2B electrodes for step changes in the oxygen concentration in either direction can be represented by a linear relation between the fractional change in the EMF and the time function exp $[-(t/\tau)^n]$. Table 2 gives values of the response time τ and the exponent n at various temperatures. The value of $n < 1$ in the exponential function probably indicates a distribution of relaxation times. The response time follows an Arrhenius-type relationship:

$$\tau = A \exp (E_{act}/RT) \quad (1)$$

Arrhenius plots for τ are shown in Fig. 8. The

Table 1. Peak height and delay time for PtU2B/yttria–zirconia/sputtered Pt (0.4 μm thick) cells

Heat treatment for sputtered Pt (0.4 μm thick) in 100% oxygen	*Peak height (mV)*				*Delay time (s)*			
	450° C		*500° C*		*450° C*		*500° C*	
	A	D	A	D	A	D	A	D
600° C (100 h)	+2.7	−4.7	+2.5	−5.0	1.6	4.8	2.1	4.6
750° C (75 h)	+30.3	−13.5	+25.9	−18.3	3.7	5.0	2.6	3.5
900° C (50 h)	+32.6	−19.7	+32.2	−18.8	5.0	7.0	3.3	4.8

A: 1 to 21% and D: 21 to 1% step change in oxygen concentration. Theoretical EMF at 450° C: 47.42 mV and at 500° C: 50.70 mV.

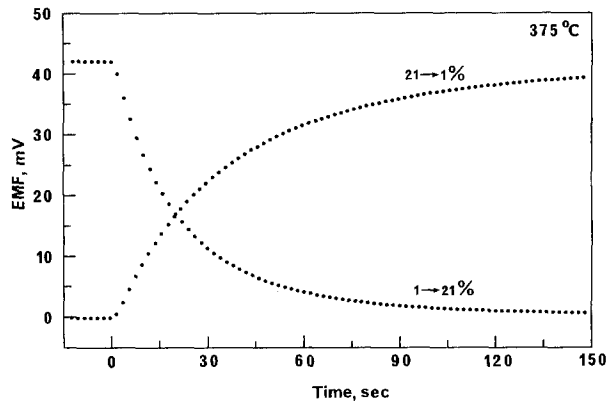

Fig. 7. Response curves for a Nernstian sensor with PtU2B electrodes, subjected to oxygen concentration changes from 21 to 1% and 1 to 21%. Air was used as the reference gas at the external electrode.

activation energies for step changes in the oxygen concentration from 21 to 1% and 1 to 21% were similar but the pre-exponential terms were different. At all temperatures the response times for step changes in the oxygen concentration from 21 to 1% were twice those obtained when the oxygen concentration was changed from 1 to 21%. The different values of the pre-exponential term may explain the asymmetry observed in the EMF–time curves when the oxygen concentration was changed from 1 to 21% and 21 to 1%. From these results it appears that oxygen uptake (1 to 21% oxygen concentration change) and oxygen release (21 to 1% change) at the electrode/electrolyte interface follow the same electrochemical path.

4.3. *Two-burner response technique*

Typical response curves obtained with the two-burner assembly are shown in Fig. 9 for two sensors, one provided with porous platinum (curves a and b) and the other with PtU2B electrodes (curves c and d). The response of both sensors, as evaluated from EMF versus time curves, was invariably faster when the gas atmosphere was changed from lean to rich (curves a and c) than for the rich to lean gas composition change (curves b and d). The reason for this asymmetry, which is reduced if the data are plotted as oxygen partial pressure versus time [14], is not clear.

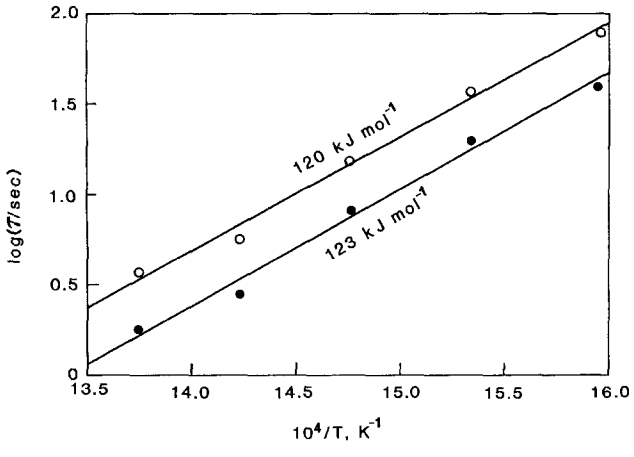

Fig. 8. Arrhenius plots for the response time of the PtU2B electrodes (Table 2). Activation energies are shown on the plots.

Table 2. Response times for a Nernstian sensor with PtU2B electrodes

Temperature (°C)	*Oxygen concentration step change*					
	1 to 21%			*21 to 1%*		
	τ (s)	n	*% error of fit*	*τ (s)*	n	*% error of fit*
354	39.8	0.78	1.4	78.9	0.74	0.9
379	19.9	0.76	1.0	37.1	0.74	0.9
404	8.2	0.76	1.3	15.4	0.75	0.6
430	2.8	0.76	1.7	5.7	0.76	0.5
454*	1.8	0.76	–	3.7	0.83	1.1

* Uncertainty due to gas front mixing.

The response time decreased rapidly as the temperature was increased. The effect of temperature is too great to be consistent with gas boundary layer diffusion as the process controlling the response rate. This contradicts the conclusions drawn by Anderson and Graves [14] who studied the response at one temperature only (600° C). An explanation involving an electrochemical step at or near the electrode/electrolyte interface (e.g. Ref. [6]) seems likely to be more appropriate.

The response rate of the sensor is influenced by many factors. Apart from the temperature and the

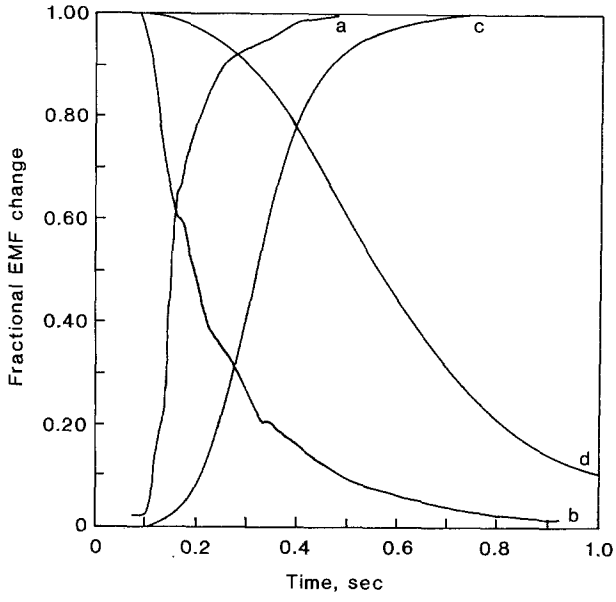

Fig. 9. Experimental response curves obtained using the two-burner technique. (a) $SIRO_2$ high temperature sensor with porous platinum electrodes. Initial air/fuel ratio 1.078, final air/fuel ratio 0.973. Sensor temperature 724° C. (b) Sensor as in curve (a). Initial air/fuel ratio 0.948, final air/fuel ratio 1.001. Sensor temperature 739° C. (c) $SIRO_2$ low temperature sensor with PtU2B electrodes. Initial air/fuel ratio 1.303, final air/fuel ratio 0.901. Sensor temperature 520° C. (d) Sensor as in curve (c). Initial air/fuel ratio 0.967, final air/fuel ratio 1.185. Sensor temperature 530° C. Note: Fractional change in the EMF has been plotted versus time with air at the reference electrode.

direction of air/fuel ratio change (lean to rich or vice versa), the response rate depends on the chemical and physical nature of the sensing electrode and the actual values of the initial and final air/fuel ratios. In particular changes from one lean mixture to another are much slower than changes across the stoichiometric air/fuel ratio.

5. Conclusions

The techniques discussed in this paper range from providing direct comparison of the response behaviour of various electrodes in clean laboratory atmospheres to a test closer to the actual use of the sensors in industrial environments. The PtU2B electrode, developed for low temperature sensor applications, responded to step changes in gas composition faster than most of the commonly used porous platinum electrodes.

Acknowledgements

The authors are thankful to W. G. Garrett for many constructively intensive discussions.

References

[1] S. P. S. Badwal, F. T. Ciacchi and W. G. Garrett, *Solid State Ionics*, accepted for publication.
[2] J. E. Anderson and Y. B. Graves, *J. Electroanal. Chem.* **133** (1982) 323.
[3] J. Fouletier, H. Seinera and M. Kleitz, *J. Appl. Electrochem.* **4** (1974) 305.
[4] J. Mizusaki, K. Amano, S. Yamauchi and K. Fueki, *J. Chem. Soc. Japan* **6** (1985) 1160.
[5] A. J. A. Winnubst, A. H. A. Scharenborg and A. J. Burggraaf, *J. Appl. Electrochem.* **15** (1985) 139.
[6] C. T. Young and J. D. Bode, SAE Technical Paper No. 790143 (1979).
[7] H. M. Wiedenmann, L. Raff and R. Noack, SAE Technical Paper No. 840141 (1984).
[8] S. Soejima and S. Mase, SAE Technical Paper No. 850378 (1985).
[9] M. J. Bannister and G. A. Hooshmand, Proc. Third Conf. on Control Engineering Sydney, 12–14 May, The Institution of Engineers, Australia (1986).
[10] S. P. S. Badwal, M. J. Bannister and W. G. Garrett, 'Advances in Ceramics; Vol. 12', The Am. Ceram. Soc., Columbus, Ohio (1984) p. 598.
[11] S. P. S. Badwal, M. J. Bannister and W. G. Garrett, *J. Phys. E.: Sci. Instr.* **20** (1987) 531.
[12] S. P. S. Badwal, F. T. Ciacchi and D. K. Sood, *J. Mater. Sci.* **21** (1986) 4035.
[13] S. P. S. Badwal, F. T. Ciacchi and D. K. Sood, *Solid State Ionics* **18/19** (1986) 1033.
[14] J. E. Anderson and Y. B. Graves, *J. Appl. Electrochem.* **12** (1982) 335.